

Measuring whole-body inert gas uptake and washout during submersion

Oscar Plogmark^{1,2}, Kristian Soltesz³, Carl Hjelte^{1,2,4}, Oskar Frånberg^{1,5}

¹ Lund University, Faculty of Medicine, Department of Clinical Sciences Lund, Respiratory Medicine and Allergology, Lund, Sweden

² Swedish Armed Forces Diving and Naval Medicine Center, Swedish Armed Forces, Karlskrona, Sweden

³ Lund University, Faculty of Engineering, Department of Automatic Control, Lund, Sweden

⁴ Kungälv Hospital, Department of Anesthesia and Intensive care, Kungälv, Sweden

⁵ Blekinge Institute of Technology, Department of Mathematics and Natural Science, Karlskrona, Sweden

Corresponding author: Dr Oscar Plogmark, Sölvegatan 19, 221 85 Lund, Sweden

ORCID: [0009-0008-3230-8807](https://orcid.org/0009-0008-3230-8807)

oscar.plogmark@med.lu.se

Keywords

Decompression sickness; Diving research; Gas kinetics; Nitrogen; Physiology; Pressure

Abstract

(Plogmark O, Soltesz K, Hjelte C, Frånberg O. Measuring whole-body inert gas uptake and washout during submersion. *Diving and Hyperbaric Medicine*. 2026 30 June;56(2):137–147. doi: [10.28920/dhm56.2.137-147](https://doi.org/10.28920/dhm56.2.137-147). PMID: [42290573](https://pubmed.ncbi.nlm.nih.gov/42290573/).)

Introduction: Quantifying inert gas uptake and washout is critical for understanding decompression sickness (DCS). However, the limited amount of data has made it difficult to integrate inert gas kinetics into risk models for DCS. Measuring whole-body inert gas kinetics during submersion is technically challenging. This study presents a novel method for quantifying inert gas uptake and washout in human divers using a rebreather-based system.

Methods: During constant-depth diving with a closed-circuit system that maintains a constant oxygen partial pressure, changes in buoyancy will reflect the kinetics of inert gas. Two divers completed four dives each, with a bottom phase at 2.5 bar and a decompression phase at 1.3 bar or 1.4 bar. Load cell data were converted into equivalent changes in volume of nitrogen standardised for temperature and pressure (V_{N_2} , STP). Power analysis was conducted to quantify the resolution by which the method could detect nitrogen uptake and washout volumes.

Results: Distinct uptake and washout curves were obtained, comparable to previous studies using other techniques. Mean V_{N_2} uptake during the bottom phase was 0.96 L (SD 0.29), while mean washout during decompression was 0.67 L (SD 0.26). The minimal mean detectable difference (MDD) with eight dives was 0.28 L for the bottom phase and 0.26 L for the decompression phase, considering standard 80% power and a 0.05 significance level.

Conclusions: This novel method quantifies inert gas kinetics during submersion with acceptable precision and accuracy. It could facilitate the collection of inert gas kinetics data during submersion, potentially yielding valuable correlations with the risk of DCS.

Introduction

Quantifying the uptake and washout of inert gases is likely a crucial component in elucidating the pathophysiology of decompression sickness (DCS).¹ While hyperbaric exposure and physiological state influence inert gas kinetics, our understanding of these processes remains limited. This knowledge gap constrains our ability to assess individual susceptibility to DCS.

Research over the years has accumulated knowledge on inert gas kinetics,^{2–13} and its association with decompression sickness (DCS).^{7,9} However, to incorporate inert gas kinetics to increase predictive accuracy in our risk models or to individualise ongoing decompression, substantially more data is required.

Due to the technical complexity of the required equipment, the number of trials measuring inert gas in the context

of diving is limited. To our knowledge, a very limited number of research groups have studied and published on techniques of measuring whole-body inert gas washout and/or uptake.^{2,8,10–12}

We recently published a proof-of-concept study on a simple setup that uses rebreather components to measure inert gas washout.⁸ This system could, in principle, also be used to assess inert gas kinetics during dives. However, its application in hyperbaric chambers is limited by regulatory requirements, increasing measurement errors at higher pressures, and the need to keep the apparatus dry inside the chamber. These factors present a significant practical challenge.

The aim of this study was to present a novel method for quantifying inert gas uptake and washout during submersion and evaluate its performance with human divers.

Methods

The study protocol was approved by the Swedish Ethical Review Authority (Dnr: 2020–06865).

DIVE PROTOCOL

Experiments were conducted in an 18 m deep tank with water maintained at 35.5°C. Each dive followed a standardised protocol. The diver wore swim trunks, a rebreather unit (Poseidon Se7en with a firmware modification that restricted the unit to only inject metabolic oxygen, disabled injections of diluent as well as extra gas injections for sensor calibration), a buoyancy control device (BCD), and adequate weights to maintain consistent negative buoyancy. Before the dive, the diver conducted a pre-dive system check in accordance with the rebreather manufacturer's guidelines. After entering the water, the diver breathed on the closed circuit at a P_{O_2} setpoint of 0.5 bar for two minutes before descent.

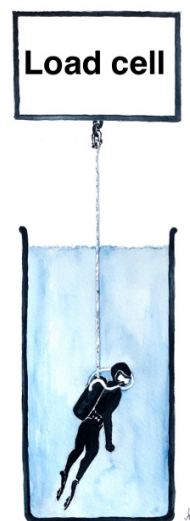
The diver emptied the BCD bladder entirely and descended passively, feet first, until restrained by the tethered line connected with the load cell (Mecmesin S-200N, Mecmesin AFTI load cell amplifier and Mecmesin VectorPro Lite logger v0.2), as shown in Figure 1. A remotely actuated crane system adjusted the line to maintain a depth corresponding to 250 kPa (2.5 bar) ambient pressure. At this depth, the diver stabilised breathing conditions by taking deep inhalations, triggering the automatic diluent valve (ADV) to partially fill the breathing circuit. Once stable, load cell measurements commenced, with the diver completely motionless and breathing normally. Only oxygen was injected into the breathing circuit during the measurement phase. These injections were actuated by the onboard P_{O_2} controller of the rebreather to compensate for metabolic consumption and thus maintain the 0.5 bar P_{O_2} setpoint.

The diver maintained this position for 25 min, during which load cell measurements were recorded. The diver then adjusted the P_{O_2} setpoint to 0.7 bar and ascended to a decompression depth with corresponding ambient pressure of 130 kPa (1.3 bar) or 140 kPa (1.4 bar). At this depth, the diver was again tethered to the load cell. Upon stabilising breathing conditions, a second 25 min load cell measurement series was recorded. The P_{O_2} setpoint change was executed before the ascent to decrease stabilisation time. The reason for increasing P_{O_2} in the first place was to establish an increased gradient between tissues and breathing gas, to accelerate decompression, translating into a higher washout rate to facilitate estimation of whole-body inert gas washout.

Throughout all load cell data collection, the operator continuously monitored the diver via in-pool camera, to ensure the absence of bubble release, confirming the

Figure 1

Experimental setup: submerged closed-circuit rebreather diver suspended from load cell



integrity of the closed rebreather system. A detailed protocol description is provided as *[Appendix A](#).

VOLUME BALANCE MODEL

A system comprising a rebreather and diver, suspended from a load cell as shown in Figure 1, experiences a buoyant force that increases linearly with the volume of water that the system displaces. For an initial time, this displacement volume can be denoted $V_o = V(t_o)$. If we are only considering changes in buoyancy, we can, without loss of generality, shift our time and volume scales, and thus defining $t_o = 0$ and $V_o = 0$. For any subsequent time $t > 0$, volume balance gives us that new displacement volume $V(t)$ is given by

$$V = V_{N_2} + V_{O_2,i} - V_{O_2,m} + V_d + V_o + V_b - V_l$$

Eq.1

where we have dropped the time argument (t) of each term, to improve readability. The meaning of each term is summarised in Table 1. To facilitate interpretation, a detailed schematic of the experimental setup is shown in Figure 2.

Some of these volume changes can be negative, namely V , V_{N_2} , V_o and V_b . For V_{N_2} , a negative value corresponds to uptake (by the diver from the circuit); a positive value corresponds to washout (from the diver into the circuit). Similarly, $V_b < 0$ corresponds to purged gas from any variable-volume.

Note that neither pressure drops in onboard oxygen or diluent cylinders affect the displacement volume, as the cylinders are fixed volume. Furthermore, gas molecules leaving the

*Footnote: Appendix A is available online on our website: <https://www.dhmjournal.com/index.php/journals?id=417>

Table 1

Definition of terms used for volumes included in Equation 1

Symbol	Explanation
V	Change in total displacement volume
V_{N_2}	Volume of physiologically bound nitrogen (inert gas) that has been washed out into the respiratory circuit
$V_{O_{2,i}}$	Volume of oxygen injected into the circuit
$V_{O_{2,m}}$	Volume of metabolised oxygen
V_d	Volume of diluent injected into the circuit
V_o	Change in volume of other gases present in the circuit (mainly carbon dioxide)
V_b	Volume added to variable-volume buoyancy compensation devices (e.g., drysuit or vest)
V_l	Volume leaked from the circuit

cylinders into the circuit, or passing between the diver and the circuit, do not contribute to any buoyancy change as the molecules remain within the suspended system. The same holds for carbon dioxide molecules being scrubbed from the circuit, by chemically binding into the scrubber material.

All volumes are reported as standard temperature and pressure (STP) equivalents in the unit of liters.

ASSUMPTIONS

In this we go through assumptions made in modeling, leading to our proposed estimation model.

Oxygen injection ($V_{O_{2,i}}$)

Oxygen injection volume, $V_{O_{2,i}}$ is assumed to be proportional to solenoid valve opening time, $t_{O_{2,i}}$, with a proportionality constant, $\alpha(P)$, that varies with ambient pressure, P .

This model has previously been verified by the rebreather manufacturer, and the ambient pressure (depth)-dependent proportionality constant between $t_{O_{2,i}}$ and $V_{O_{2,i}}$ is logged by the rebreather.

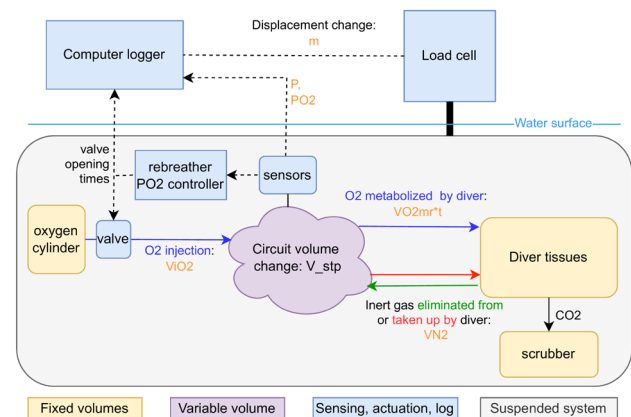
We were able to independently verify this model by noting that the magnitude of jumps in V registered by the load cell at each oxygen injection instance matched those predicted by the model.

Oxygen metabolism ($V_{O_{2,m}}$)

Oxygen metabolic rate, $V_{O_{2,m}}$ is assumed to be constant throughout each measurement series. With the diver at complete rest while suspended from the load cell, this

Figure 2

Schematic overview of system components, gas flows, and signals



assumption is plausible. Its validity was verified for our measurements by inspection of the logged high-pressure gauge connected to the oxygen cylinder, and the cumulative solenoid valve opening time. During episodes of stable P_{O_2} , both these lines featured a constant slope.

Diluent injection (V_d)

The intention was to avoid diluent injections altogether, corresponding to $V_d = 0$. However, if the rebreather circuit is breathed down to a level that activates the mechanical ADV, a distinct jump in V results analogous to that caused by a solenoid valve oxygen injection. By manually determining the magnitude of any such jumps, it is possible to estimate the volume of injected diluent.

Influence of other gases (V_o)

To estimate V_{N_2} based on Equation 1, the volume change contribution from other gases, V_o , needs to be known. These gases are mainly carbon dioxide, water vapor, and traces of other inert gases, such as argon. Assuming adequate carbon dioxide scrubbing and measuring P_{O_2} after the scrubber, it is justified to neglect the effect of carbon dioxide fraction (fluctuation) on the total circuit volume V . Similarly, the fraction of other inert gases is typically sufficiently low within the respiratory circuit to be safely neglected.

Although water vapor in the respiratory circuit may fluctuate due to temperature changes and moisture production from both the diver and the carbon dioxide scrubber, these variations are negligible. At 37°C and 250 kPa (2.5 bar), the vapour pressure of water (≈ 6 kPa [0.06 bar]) is insignificant compared to oxygen and nitrogen pressures. Thus, water vapor can be excluded from analysis without significantly affecting measurement accuracy or precision.

To summarise, we have made the simplifying assumption that $F_{O_2} + F_{N_2} = 1$ within the circuit at all times.

Buoyancy compensation (V_b)

We assume $V_b = 0$, which is easy to confirm, simply by not manually adjusting buoyancy by gas injection into variable volumes (other than metabolic oxygen injection into the respiratory circuit).

Leaks (V_l)

We assume $V_l = 0$, which is easy to confirm by visual monitoring to assure no bubbles leave the diver during an ongoing measurement series. This was done during all reported measurement series.

Temperature effects

Under the ideal gas law, the volumes of Equation 1 scale linearly with absolute temperature. Such effect can be eliminated by conducting the experiment in water that holds a constant, known temperature. While our rebreather setup lacked circuit temperature monitoring, the dives were conducted in a pool with fresh water holding a constant temperature. We thus assume a constant circuit temperature, T_c , throughout each experiment series.

Inert gas kinetic time scale

While breathing on the circuit, the centre of mass of the diver shifts slightly as gas moves between lungs and counter lungs. This induces oscillations in the load cell measurement of a diver suspended according to Figure 1. While it might be possible to compensate for such oscillations, our approach has been to instead only consider inert gas kinetics at a time scale slower than that of the respiratory dynamics. This introduces a trade-off between frequency resolution and noise penetration, and we have chosen to disregard any estimated signal components corresponding to a time scale faster than a five-minute half-time, being a commonly used fastest half-time in decompression models.^{1,13}

Sweating

The careful reader might have noticed that Equation 1 only concerns gas volume changes. While the diver might change weight, mainly due to sweating, the impact of such weight change is negligible as the densities of sweat and surrounding water are very similar, with a relative difference of around 1–3% (depending on the combination of salt content in the sweat and surrounding water). We therefore neglect the effect of sweating on change in buoyancy.

ESTIMATION MODEL

In this section we combine the fundamental volume balance of Equation 1 with the assumptions of Section

“ASSUMPTIONS”, to arrive at a model for estimation of V_{N_2} from available measurements:

$$V_{N_2} = V - V_{O_{2,i}} + V_{O_{2,m}} \quad \text{Eq.2}$$

Equation 2 merely states that at any time during ongoing measurement, the change in physiologically bound nitrogen volume is the difference between the total volume change, V , compensated by the volume change due to injected oxygen $V_{O_{2,i}}$ and stabilising oxygen $V_{O_{2,m}}$, respectively. As already stated, we consider all volumes as their STP equivalents.

Next, we construct estimators for each of the right-hand-side terms, to arrive at an estimator for the desired left-hand-side of Equation 2. The term V is readily available by scaling the load cell reading using the ideal gas law, as described in Section “Total volume change estimation”.

Oxygen is injected in bursts, and since the onset and duration of the oxygen-injecting solenoid valve activations are logged by the rebreather, we know when these bursts occur, and how long they each last. What remains is to determine the resulting volumes of injected oxygen, being the topic of Section “Oxygen injection estimation”.

Oxygen metabolic rate was constant throughout each measurement series. In Section “Oxygen metabolic rate estimation” this constant metabolic rate is estimated, taking into account both that there is a transient at the beginning of each measurement phase, and that mean oxygen injection rate does not exactly match metabolic rate. The former is caused by the rebreather stabilising P_{O_2} following a change in depth. The latter is a consequence of more or less oxygen needed in the circuit to maintain a stable P_{O_2} as the circuit nitrogen content changes due to diver uptake and washout.

Before moving on, we can also note that despite the total flux of oxygen through the system (roughly $V_{O_{2,i}}(t)/t$) being an order of magnitude larger than the quantity V_{N_2} of interest to us, we can still enable reliable estimates. This is because the system is open to oxygen, but closed to inert gas, as pointed out and further explained elsewhere.¹³

An error analysis of the resulting estimation model is provided in Section “Error analysis”.

Total volume change estimation

We use the change in load cell measurement, m , in combination with the ideal gas law, to estimate the change in circuit volume:

$$\hat{V}(t) = \frac{T_0 \dot{P}}{\hat{T}_c P_0} m(t) \quad \text{Eq.3}$$

where $T_0 = 273.15$ K and $P_0 = 1.01325$ bar (1 atmosphere) are the STP temperature and pressure, respectively. Since the diver is suspended by a static line of known length, the ambient pressure can be considered known with certainty, $\widehat{P} = P$.

All dives were conducted in a heated pool, holding a constant temperature of 35.5°C , close to normal physiological human core body temperature of 37°C . It is fair to assume that heat loss from the circuit to the water balances heat introduced by the exothermic scrubber reaction. We have therefore assumed a mean circuit temperature of $T_c = T_0 + 37^\circ\text{C}$ throughout all measurement series.

Oxygen injection estimation

The estimate of (cumulative) volume of oxygen injected into the circuit is:

$$\hat{V}_{O_2,i}(t) = \int_0^t \alpha(P(\tau)) \mathbb{1}_{O_2,i}(\tau) d\tau = \alpha(P) \int_0^t \mathbb{1}_{O_2,i}(\tau) d\tau = \alpha(P) t_{O_2,i}(t) \quad \text{Eq.4}$$

The pressure-dependent injection rate $\alpha(P)$ is constant throughout the measurement phase, as the diver is suspended at a fixed depth, thus exposed to a constant ambient pressure, P . Hence, we can move $\alpha(P) = \alpha(P(t))$ outside the integral. The indicator $\mathbb{1}_{O_2,i}(t)$ is 1 for t when the oxygen solenoid valve is open, and 0 otherwise, and thus integrates up to the total solenoid valve opening time, $t_{O_2,i}(t)$.

As mentioned in elsewhere, it was possible to verify the correctness of the manufacturer-supplied injection rate constant $\alpha(P)$, by confirming that compensation through Equation 4 exactly cancels the injection jumps. These jumps are thus visible in the raw load cell signal shown in the black top pane plots of Figure 3, but not in the corresponding compensated light red V_{N_2} estimates in the second topmost panes.

Oxygen metabolic rate estimation

Following an initial transient caused by the change in depth preceding each measurement series, the onboard partial pressure controller of the rebreather stabilised the P_{O_2} at its setpoint. Since ambient pressure, P , is constant during a measurement series, and known with certainty as the diver is suspended by a static line, this also means that F_{O_2} is stabilised. We use the average as an estimate of the stabilised F_{O_2} , where \widehat{P}_{O_2} is the reading from the primary oxygen partial pressure sensor, and \widehat{P}_{O_2} denotes its average between time instances t_1 and t_2 .

$$\hat{V}_{O_2,m} = \frac{\hat{V}_{O_2,i}(t_2) - \hat{V}_{O_2,i}(t_1) + \hat{V}_{O_2,c}(t_2, t_1)}{t_2 - t_1} = \frac{\alpha(P) (t_{O_2,i}(t_2) - t_{O_2,i}(t_1)) + \frac{\widehat{P}_{O_2} T_0}{P_0 \widehat{T}_c} (m_f(t_2) - m_f(t_1))}{t_2 - t_1} \quad \text{Eq.5}$$

Eq.5

We can now use our stable oxygen fraction estimate, \widehat{F}_{O_2} of Equation 5 to estimate the volume of injected oxygen between t_1 and t_2 , $V_{O_2,c}(t_2, t_1)$ that remains in (or is metabolised from, in case of $V_{O_2,c} < 0$) the circuit at t_2 :

$$\hat{V}_{O_2,c}(t_2, t_1) = \widehat{F}_{O_2} (\widehat{V}_f(t_2) - \widehat{V}_f(t_1)) \quad \text{Eq.6}$$

The subscript f , as in \widehat{V}_f of Equation 6, denotes that the underlying \widehat{V} signal has been low-pass filtered to remove the respiratory-induced noise mentioned in Section “*Inert gas kinetic time scale*”.

Combining Equations 4 to 6, we thus arrive at the metabolic rate estimator:

$$\hat{V}_{O_2,m} = \frac{\hat{V}_{O_2,i}(t_2) - \hat{V}_{O_2,i}(t_1) + \hat{V}_{O_2,c}(t_2, t_1)}{t_2 - t_1} = \frac{\alpha(P) (t_{O_2,i}(t_2) - t_{O_2,i}(t_1)) + \frac{\widehat{P}_{O_2} T_0}{P_0 \widehat{T}_c} (m_f(t_2) - m_f(t_1))}{t_2 - t_1} \quad \text{Eq.7}$$

INERT GAS LOADING ESTIMATOR

Combining Equations 2 to 4 and 7, we finally arrive at the inert gas uptake/washout estimator:

$$\hat{V}_{N_2}(t) = \hat{V}(t) - \hat{V}_{O_2,i}(t) + \hat{V}_{O_2,m}(t) = \frac{T_0 P}{\widehat{T}_c P_0} m(t) - \alpha(P) t_{O_2,i}(t) + \frac{\alpha(P) (t_{O_2,i}(t_2) - t_{O_2,i}(t_1)) + \frac{\widehat{P}_{O_2} T_0}{P_0 \widehat{T}_c} (m_f(t_2) - m_f(t_1))}{t_2 - t_1} t \quad \text{Eq.8}$$

Subsequently, we apply low-pass filtering to remove respiratory-induced artifacts, arriving at the final estimator $\widehat{V}_{N_2,f}$.

IMPLEMENTATION

For each dive, time series logs of m , P_{O_2} , and $t_{O_2,i}$ were time-aligned and re-sampled at a rate of 1 Hz. This resampling was performed in a way that preserved oxygen solenoid valve activation time. Remaining signals were linearly re-sampled, except oxygen partial pressure setpoint, which was resampled to nearest neighbor.

While we used integrals in Section “*ESTIMATION MODEL*” for generality, the corresponding zero-order-hold sampled sums were used in the code implementing our estimator, as we only have access to measurements at discrete sampling instances.

Figure 3

Each of the sub-figures (1–8) represent one dive. Odd sub-figures correspond to dives made by Diver 1; even sub-figures to dives made by Diver 2. The top panel of each sub-figure shows ambient pressure in black, and load cell raw measurement (affinely transformed to V_{N_2}) in light blue. A version of the latter, compensating for oxygen injections and constant oxygen metabolic (mass) rate is shown in light red. The bright red curve is obtained from the light red curve through low-pass filtering. Finally, the bright blue curve is a simulation of the one-compartment model that best fits the light red curve, in the least-squares sense. The mid panels show P_{O_2} measurements from the rebreather in black. The light red spikes show activation times of the solenoid valve that injects oxygen into the breathing circuit. The bottom panels show oxygen cylinder gauge pressure in grey. The black lines are isotonic regressions of the noisy pressure measurement during the bottom and decompression stages. The cumulative sum of solenoid valve opening times is shown in red

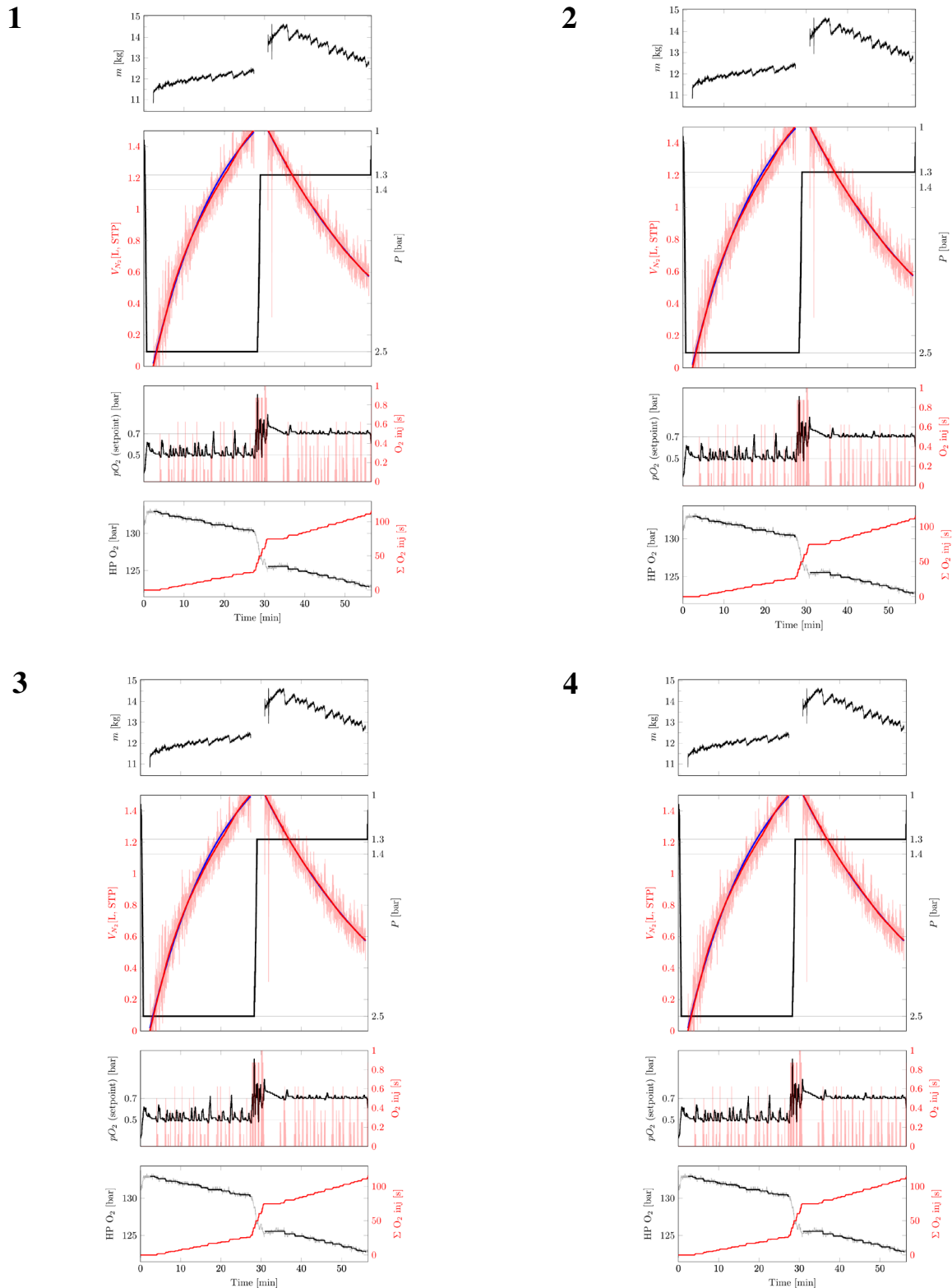
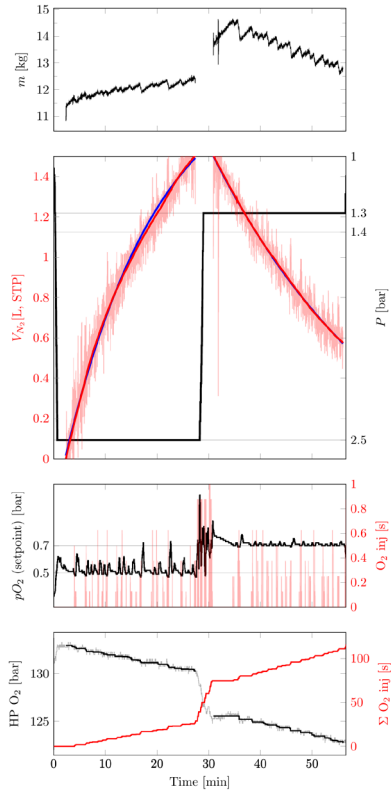
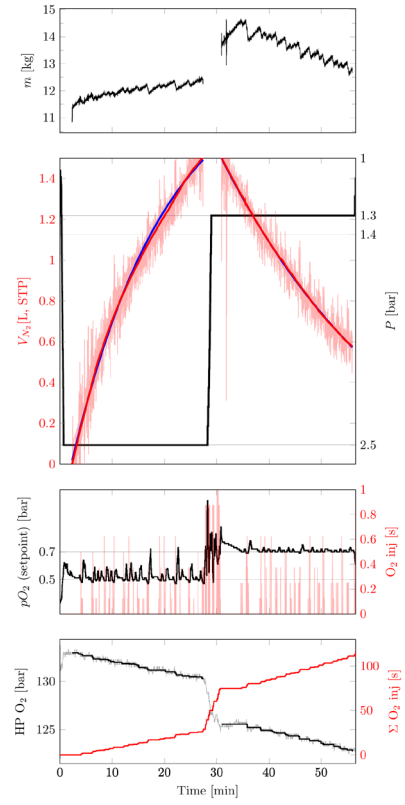


Figure 3 continued.
Sub figures 5–8

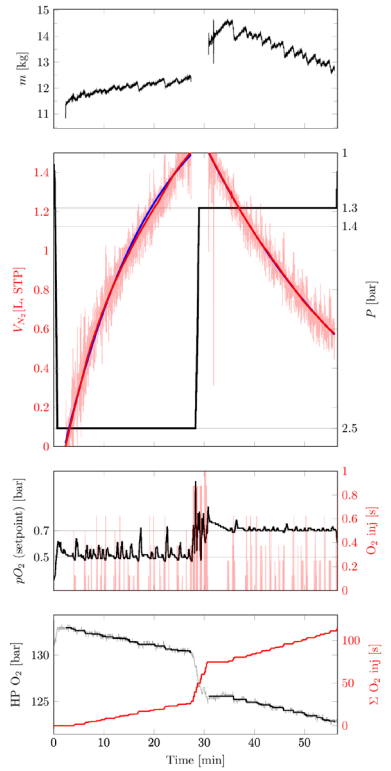
5



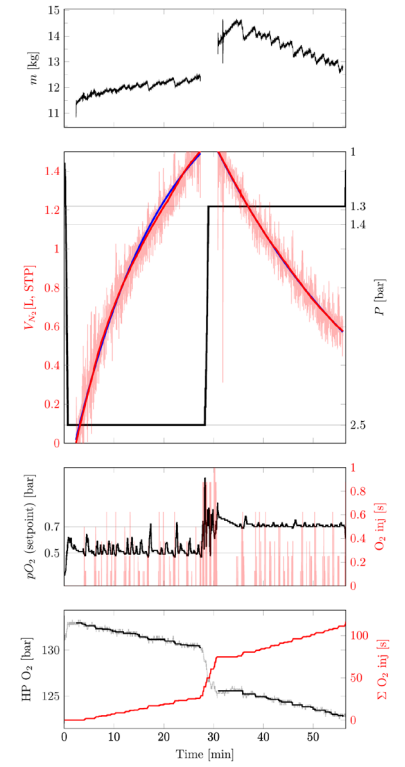
6



7



8



The mentioned low-pass filtering was achieved using an acausal moving average filter of window width $T_f = 5/\ln(2)$ min, matching the -3 dB cutoff of a first-order low-pass filter with 5min time constant. To avoid edge-effect artifacts, an exponential model extrapolation was used as padding.

For further details, please see the estimation code used in the study, provided in *Appendix B.

ERROR ANALYSIS

In this section we discuss possible sources of error, and their impact on the estimate $\widehat{V}_{N_2,f}$.

Ambient pressure (P)

Ambient pressure enters the estimator of Equation 8 linearly in the \widehat{V} term. Thus, an error in its measurement will have an affine impact on \widehat{V} .

Since the diver was suspended in a static line of known length, we can consider errors in ambient pressure measurement as negligible and assert $\widehat{P} = P$ throughout each measurement series.

Suspended mass (m)

An error in mass measurement affects the estimate mainly by its linear impact on \widehat{V} , but also slightly by its linear impact on the estimated circuit oxygen volume change $\widehat{V}_{O_2,c}$, that appears affinely in the term $\widehat{V}_{O_2,m}$. An error in the measurement thus has an affine impact on \widehat{V}_{N_2} , with an induced error that is less than proportional to the error in m .

Since we deal only with differential measurements (between $t = 0$ and subsequent $t > 0$), taring error can be neglected, and the amount of drift of the load cell over the considered measurement durations is negligible.

Circuit temperature (T_c)

Error in the circuit temperature estimate \widehat{T}_c propagates to \widehat{V}_{N_2} the same way as error in m , with a sub-proportional impact.

Letting $T_c = \widehat{T}_c + \varepsilon$, we have a relative error factor $T_c/\widehat{T}_c = 1 + \varepsilon/\widehat{T}_c$. Even with an over-estimation of this error, with a value as high as $\varepsilon = 5$ °C, the relative error in \widehat{T}_c in will lie well below 2%.

Oxygen partial pressure (P_{O_2})

By far the dominating error source in our setup is the discrepancy between assumed and actual P_{O_2} . There are

two contributors to this error: deviation between measured P_{O_2} and setpoint, and deviations between measured P_{O_2} and actual P_{O_2} .

In our estimator, an average \overline{P}_{O_2} is used to estimate the oxygen metabolic rate, $\widehat{V}_{O_2,m}$, as described in Section “Oxygen metabolism ($V_{O_2,m}$)”. This mitigates the impact of deviation between measured P_{O_2} and setpoint. However, any P_{O_2} measurement error linearly impacts $\widehat{V}_{O_2,c}$, and thus has an affine impact on \widehat{V}_{N_2} .

To quantify this error, we consider Equation 8 and note that a multiplicative error ε contributes with an error:

$$\widehat{V}_{N_2}(t) - V_{N_2}(t) = \overline{P}_{O_2} \left((1 + \varepsilon) - 1 \right) \frac{T_0}{P_0 \widehat{T}_c} \frac{m_f(t_2) - m_f(t_1)}{t_2 - t_1} t \tag{Eq.9}$$

We see directly from Equation 9 that the relative error is simply:

$$\frac{\widehat{V}_{N_2} - V_{N_2}}{V_{N_2}} = \varepsilon \tag{Eq.10}$$

To gauge the corresponding absolute error, we note that the largest error will occur at the end of a measurement series, where $t = 25$ min. With a representative mass change of 1 kg and the worst-case (largest) $\overline{P}_{O_2} = 1.3$ bar we would then have:

$$\widehat{V}_{N_2}(t) - V_{N_2}(t) = \varepsilon \cdot 1.3 \frac{1}{1.01325} \frac{273.15}{273.15 + 37} \frac{25}{20} \approx 1.41 \varepsilon \tag{Eq.11}$$

Thus, in this case, a multiplicative error of 10 % would result in a 0.14 L error in the estimated total V_{N_2} of 1 L.

Unaccounted for volume changes ($V_d + V_o + V_b - V_l$)

Any unaccounted volume change will contribute directly to an error in \widehat{V}_{N_2} , as evident from Equation 1. Visual bubble monitoring and lack of BCD adjustments make it possible for us to neglect V_b and V_l . The two occasions of ADV diluent addition have been manually compensated for, as described in Section “Diluent injection (V_d)”.

The remaining error source is the volume change V_o of unaccounted gases other than oxygen and nitrogen, as already discussed in Section “Influence of other gases (V_o)”. As mentioned, this source propagates directly to the estimate \widehat{V}_{N_2} . However, as long as the volume of unaccounted gases is constant, the corresponding volume change V_o , cf. Section “Suspended mass (m)”.

*Footnote: Appendix B is available online on our website <https://www.dhmjournal.com/index.php/journals?id=417>

Table 2
Characteristics of participants; BMI – body mass index

ID	Sex	Age (Years)	Weight (kg)	Height (cm)	BMI (kg·m ⁻²)
1	Male	48	83	182	25
2	Male	47	83	180	25

Figure 4

Change in V_{N_2} STP during the bottom and deco stage of each dive; dives by Diver 1 are shown in blue and by Diver 2 in red

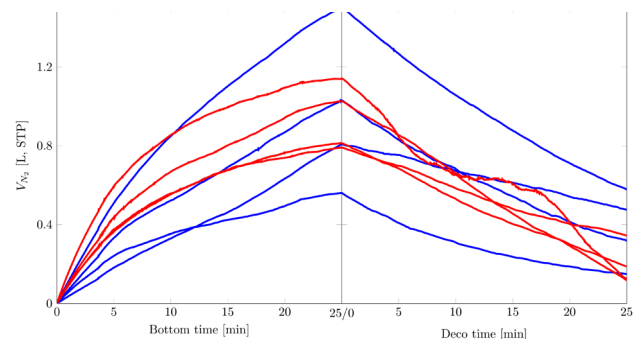


Table 3

Bottom phase nitrogen uptake, decompression phase washout and the difference thereof (L, STP), reported for each of eight dives conducted by the two divers; last row shows mean and standard deviation (SD) across all dives

Dive	Diver	Bottom V_{N_2}	Deco V_{N_2}	Sum V_{N_2}
1	1	1.50	-0.93	0.58
2	2	1.14	-1.02	0.13
3	1	1.03	-0.71	0.32
4	2	0.79	-0.45	0.34
5	1	0.56	-0.41	0.15
6	2	1.03	-0.91	0.12
7	1	0.81	-0.33	0.47
8	2	0.81	-0.63	0.19
Mean (SD)		0.96 (0.29)	-0.67 (0.26)	0.29 (0.17)

Results

Two divers (Table 2), completed four dives each, with a bottom phase at 250 kPa (2.5 bar) and a decompression phase at either 130 kPa (1.3 bar) or 140 kPa (1.4 bar) (Diver 1: one dive at 1.4 bar; Diver 2: three dives at 1.4 bar). Uptake and washout of nitrogen from each dive exhibited distinct curves, with intra- and interindividual variability comparable to findings from previous inert gas kinetic measurement techniques,^{4,6,8,10} (see Figures 3 and 4).

Mean N_2 uptake during the bottom phase was 0.96 L (SD 0.29), and mean washout during decompression was 0.67 L (SD 0.26), see Figures 3 and 4 and Table 3. The figure and table ordering are identical.

The nitrogen loading volumes, obtained from load cell measurements of buoyancy differences during the 25 min bottom and 25 min decompression phases, were consistent with physiologically expected quantities.^{14,15}

According to Gabler-Smith et al.,¹⁴ the solubility of nitrogen in human adipose tissue is approximately $\alpha = 61 \cdot 10^{-2}$ mL gas per mL solvent under standard physiological temperature (37°C) and pressure (1 bar). Using the ideal gas law, Henry's constant is given by $k_H = \alpha/(RT)$. Substituting $R = 0.08314$ L bar⁻¹mol⁻¹°K⁻¹ and $T = 310.15$ °K yields $K_{H,a} = 2.37 \cdot 10^{-3}$ mol·bar⁻¹L⁻¹ for adipose tissue. For lean tissue, the corresponding value is $k_{H,l} = 4.7 \cdot 10^{-4}$ mol·bar⁻¹L⁻¹.¹⁵

Assuming a total body mass of $m = 83$ kg, being the weight of both the divers, with approximate adipose fraction $F_a = 25\%$. Transitioning from breathing air at the surface to a nitrox mixture with $P_{O_2} = 0.5$ bar at a depth corresponding to 2.5 bar total pressure, the diver is expected to absorb 1.78 L of nitrogen before reaching equilibrium. The measured buoyancy differences during 25 min bottom and 25 min decompression phases thus aligned with theoretical predictions.

Power analysis (with $\alpha = 0.05$ and 80% power) indicated that the minimal detectable mean difference (MDD) in V_{N_2}

uptake and washout for $n = 8$ dives was 0.28 L, and 0.26 L, for bottom and deco phase, respectively.

Discussion

MAIN FINDINGS

We present a novel method for quantifying nitrogen (inert gas) uptake and washout during submersion. Evaluation in human subjects demonstrated volumes consistent with expected physiological ranges.^{2,4,8,15} The approach is straightforward to implement but currently requires a controlled environment and restricts diver movement during measurement. Furthermore, the method relies on no inert gas being injected into the breathing circuit and no gas leakage during ongoing measurement.

IMPLICATIONS

The presented technique enables quantification of inter- and intraindividual variability in inert gas uptake and washout. The method may offer new insights into how uptake and washout vary with individual covariates such as body composition, age or genotype, or different physiological states such as thermal exposure, workload, or hydration.

With sufficient data, the method could potentially help elucidate correlations between inert gas uptake/washout and DCS risk. However, such applications require extensive datasets across diverse dive profiles with known DCS outcomes.

STRENGTHS AND LIMITATIONS

The proposed setup is considerably simpler than existing methods for measuring inert gas kinetics underwater.^{11,12} Its data processing pipeline effectively suppresses non-physiological fluctuations. Since these eight dives were the first using this system, bias from prior calibration or adjustment dives is avoided.

The main limitation is that no dive was performed using a nitrogen partial pressure identical to that of air at 1 bar, which would be expected to yield zero washout and zero uptake of nitrogen. Such a reference condition would have provided a stable baseline for detecting potential system drift. Additional limitations include the small sample size and the use of two decompression depths, which complicate direct comparison of outcomes. As noted in the error analysis, deviations from the PO_2 setpoint, arising from imperfect reference tracking or sensor drift, constitute the dominant source of error. Intermittent calibration using sampled gas analysis, with subsequent correction of logged PO_2 values, could mitigate the latter. Incorporation of temperature monitoring within the breathing circuit would further strengthen performance under variable thermal conditions.

Conclusions

We introduce a novel method for quantifying inert gas during submersion, demonstrating that it can achieve physiologically consistent results with adequate precision and accuracy in humans. The approach has potential to enable systematic quantification of inert gas data during diving, thereby advancing understanding of decompression physiology and the mechanisms underlying decompression sickness.

References

- 1 Brubakk AO, Neuman TS, editors. Bennett and Elliott's physiology and medicine of diving. 5th ed. Edinburgh: Saunders; 2003.
- 2 Balldin UI. Effects of ambient temperature and body position on tissue nitrogen elimination in man. *Aerosp Med.* 1973;44:365–70. [PMID: 4694843](#).
- 3 Balldin UI, Lundgren CE. Effects of immersion with the head above water on tissue nitrogen elimination in man. *Aerosp Med.* 1972;43:1101–8. [PMID: 5076612](#).
- 4 Pendergast DR, Senf CJ, Fletcher MC, Lundgren CE. Effects of ambient temperature on nitrogen uptake and elimination in humans. *Undersea Hyperb Med.* 2015;42:85–94. [PMID: 26094308](#).
- 5 Lundgren CE, Eckhardt LG, Senf CJ, Bowdwin MR, Pendergast DR. Negative pressure breathing increases cardiac output and nitrogen elimination in seated subjects. *Undersea Hyperb Med.* 2013;40:403–10. [PMID: 24224284](#).
- 6 Pendergast DR, Senf C, Lundgren CE. Is the rate of whole-body nitrogen elimination influenced by exercise? *Undersea Hyperb Med.* 2012;39:595–604. [PMID: 22400450](#).
- 7 Balldin UI. The preventative effect of denitrogenation during warm water immersion on decompression and decompression sickness in man. *First Annual Scientific Meeting of the European Undersea Baromedical Society.* 1973:239–43.
- 8 Plogmark O, Silvanus M, Olsson M, Hjelte C, Ekström M, Frånberg O. Measuring whole body inert gas wash-out. *Diving Hyperb Med.* 2023;53:321–6. [doi: 10.28920/dhm53.4.321-326](#). [PMID: 38091591](#). [PMCID: PMC10944667](#).
- 9 Gerth WA VR, Leatherman NE. Whole-body nitrogen elimination during oxygen prebreathing and altitude decompression sickness risk. *The Thirty-Eighth Undersea and Hyperbaric Medical Society Workshop.* 1989:147–51.
- 10 Dick AP, Vann RD, Mebane GY, Feezor MD. Decompression induced nitrogen elimination. *Undersea Biomed Res.* 1984;11:369–80. [PMID: 6535313](#).
- 11 Sundblad P, Frånberg O, Siebenmann C, Gennser M. Measuring uptake and elimination of nitrogen in humans at different ambient pressures. *Aerosp Med Hum Perform.* 2016;87:1045–50. [doi: 10.3357/AMHP.4680.2016](#). [PMID: 28323592](#).
- 12 Kindwall EP, Baz A, Lightfoot EN, Lanphier EH, Seireg A. Nitrogen elimination in man during decompression. *Undersea Biomed Res.* 1975;2:285–97. [PMID: 1226586](#).
- 13 Natoli MJ, Vann RD, Gerth WA. Nitrogen uptake during air diving. Final technical report (Contract No. N00014-91-J-1763). Durham, NC: Duke University Medical Center; 1994.
- 14 Gabler-Smith MK, Westgate AJ, Koopman HN. Microvessel density, lipid chemistry and N_2 solubility in human and pig

adipose tissue. *Undersea Hyperb Med.* 2020;47:1–12. doi: [10.22462/01.03.2020.25](https://doi.org/10.22462/01.03.2020.25). PMID: [32176941](https://pubmed.ncbi.nlm.nih.gov/32176941/).

- 15 Gabler-Smith MK, Westgate AJ, Koopman HN. Fatty acid composition and N(2) solubility in triacylglycerol-rich adipose tissue: the likely importance of intact molecular structure. *J Exp Biol.* 2020;223(Pt 5):jeb216770. doi: [10.1242/jeb.216770](https://doi.org/10.1242/jeb.216770). PMID: [32001545](https://pubmed.ncbi.nlm.nih.gov/32001545/).

Acknowledgements

We gratefully acknowledge the support from the Swedish Armed Forces Diving and Naval Medicine Center.

Conflicts of interest and funding

Funding was provided through unrestricted grants from the Swedish Defence Materiel Administration (430919–LB967593). Kristian Soltesz is a member of the ELLIIT Strategic Research Area at Lund University. The authors declare no conflicts of interest relevant to this work.

Submitted: 6 March 2025

Accepted after revision: 12 March 2026

Copyright: This article is the copyright of the authors who grant *Diving and Hyperbaric Medicine* a non-exclusive licence to publish the article in electronic and other forms.

Diving and Hyperbaric Medicine Journal copyright statement 2026

All articles in *Diving and Hyperbaric Medicine* are published under licence from the authors. Copyright to these articles remains with these authors. Any distribution, apart from for limited educational purposes, is in breach of copyright.